Article

pubs.acs.org/Biomac

Ultrasensitive Detection of MicroRNA in Tumor Cells and Tissues via Continuous Assembly of DNA Probe

Yuhui Liao, Yu Fu, Yunxia Wu, Ru Huang, Xiaoming Zhou,* and Da Xing*

MOE Key Laboratory of Laser Life Science & Institute of Laser Life Science, College of Biophotonics, South China Normal University; Guangzhou, China

Supporting Information

ABSTRACT: Nucleic acids have been engineered to participate in a wide variety of tasks. Among them, the enzyme-free amplification modes, enzyme-free DNA circuits (EFDCs), and hybridization chain reactions (HCRs) have been widely applied in a series of studies of bioanalysis. We demonstrated here an ultrasensitive hairpin probe-based circulation for continuous assemble of DNA probe. This strategy improved the analyte stability-dependent amplification efficiency of EFDC and signal enhancement without being limited by the analyte's initial concentration, and it was used to produce a novel microRNA (miRNA) trace analysis assay with ultrasensitive amplification properties. Through the detection of standard miRNA substances, 1 amol-level sensitivity and satisfactory specificity were achieved. Compared with EFDCs and HCRs, the sensitivity of ultrasensitive hairpin probe-based circulation was higher by 3 or 4 orders of magnitude. Furthermore, the excellent performance of this platform was also demonstrated in the detection of miRNAs in tumor cells. The sensitivities for the detection of miRNAs in HepG2, A549 and MCF-7 tumor cells were 10, 10, and 100 cells, respectively. In addition, a high detection rate of 83% was achieved for tumor tissues. Thus, this ultrasensitive hairpin probe-based circulation possesses the potential to be a technological innovation in the field of tumor diagnosis.

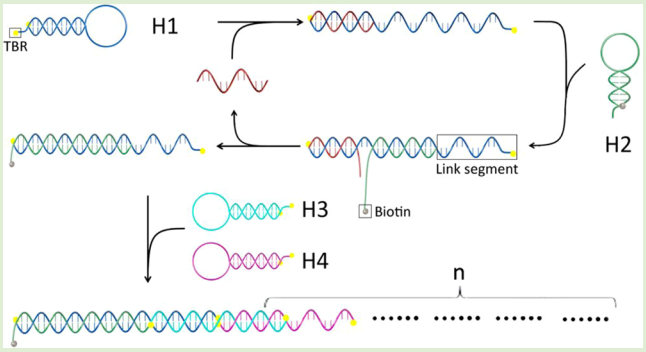

1. INTRODUCTION

As the representative biomacromolecules, nucleic acids perform significant functions in life processes.[1,2] There has been a dramatic progress in the studies regarding functions of microRNAs (miRNAs).[3−5] miRNAs are highly conserved small single-stranded RNAs with the length of 18−25 nt,[6−9] encoded by noncoding endogenous genes.[10−12] Their functional mechanism in regulation of gene expression has attracted enormous attention, since the first miRNA was reported in the early 1990s.[13] It has also been demonstrated that the expression levels of miRNAs are directly related to diverse cancers.[14−16] Thus, miRNAs possess the potential to be employed as valuable biomarkers for molecular diagnosis of tumors. However, the natural features of miRNAs, such as the small size, vulnerable degradability, similarities of the sequences, and relatively low expression levels in cells, makes quantitative analysis of miRNAs to be a tough call (especially, the miRNAs extracted from complicated conditions, such as cells, tissues, and biological fluids). Therefore, an ultrasensitive, simplified and stabilized analytical method possesses the practical and clinical significance for quantitative analysis of miRNAs.

In recent years, engineered nucleic acids have been shown to participate in a wide variety of tasks.[17−19] For example, DNAzymes initiate new catalysis patterns,[20−22] aptamers are involved in novel biological recognition events,[23,24] and catalytic hairpin assemblies achieve enzyme-free amplification patterns that are widely utilized in biosensing.[25−28] As representative enzyme-free amplification patterns, programming biomolecular self-assembly pathways have been widely applied in series assays.[29−32] Inspired by enzyme-free DNA circuits (EFDCs, a particular case of 'programming biomolecular self-assembly pathways'), we developed a target-triggered enzyme-free amplification strategy for the detection of miRNAs.[33] However, the vulnerable stability of miRNAs can adversely affect amplification efficiency. As shown in Scheme 1A, EFDCs are actuated by strand displacement and the circulation of target analytes, which should remain stable and return to the free-state within each repetition for continuation of the amplification process. Thus, the stability of the target analyte is related to the amplification efficiency. For degradable target analytes (such as miRNAs), the amplification efficiency is reduced along with the degradation of the analyte (Figure 2A). Therefore, this strategy requires a rigorous RNase-free condition throughout the entire amplification process. Furthermore, the lower sensitivity limited its application, an

Received: July 20, 2015
Revised: September 20, 2015
Published: October 13, 2015

DOI: 10.1021/acs.biomac.5b00959
Biomacromolecules 2015, 16, 3543−3551

Scheme 1. Principle of the Ultrasensitive Hairpin Probe-Based Circulation Pattern[a]

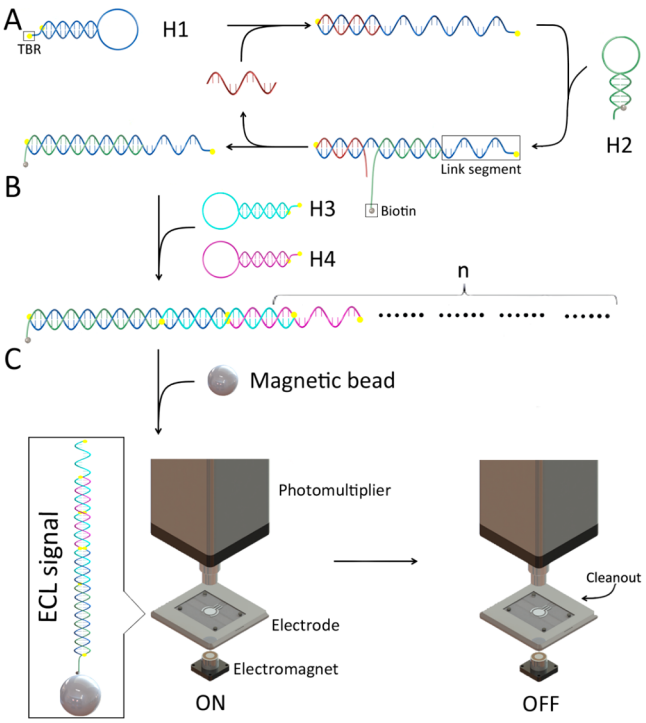

[a](A) Initial amplification step of enzyme-free DNA circuits. Both ends of H1 were labeled with $Ru(bpy)_3^{2+}$(TBR), and H2 was labeled with biotin. The link segment was exposed when the H1+H2 complex was generated. (B) Signal enhancement process for the HCR. Both ends of H3 and H4 were labeled with TBR. (C) Magnetic bead capture and ECL signal-producing steps. The magnetic beads were labeled with streptavidin, which was employed as the capture group for biotin.

unsatisfactory sensitivity around 10 fmol was achieved according to existing investigations.[34−37]

Therefore, we focused on another enzyme-free amplification pattern, hybridization chain reaction (HCR),[38−40] to obtain improved amplification efficiency for miRNAs. It is well-known that HCR can sustain the formation of DNA while the assembly process is triggered by a target (shown in Scheme 1B). In this process, the amplification efficiency does not rely on the circulation of target analytes but on the alternate self-assembly of two hairpin probes. Therefore, this process is more suitable for degradable target analytes. However, this process relies strongly on the initial concentration of analytes (Figure 2B). HCR is incapable of producing a recognizable signal when the initial concentration is sufficiently low (lower than 10 fmol), which is disadvantageous in the field of trace analysis. Thus, an evolutionary enzyme-free amplification pattern with high amplification efficiency is needed.

Herein, we integrated the EFDC and HCR processes and constructed an ultrasensitive hairpin probe-based circulation pattern for miRNA trace analysis (Scheme 1). The central purpose of this work is to construct an ultrasensitive enzyme-free amplification platform for miRNA detection. In this strategy, EFDC was employed as the foremost amplifier to produce a response with trace miRNA and convert it to a stable 'H1+H2' DNA complex at the initial amplification stage. Then, a link segment in H1 was designed to concatenate the subsequent HCR process. When the EFDC is activated, the exposed site H1 triggers the continuous HCR process, and the continuous probe-assemble of DNA was entirely triggered. This strategy utilizes the circulation of miRNA in the initial amplification stage, which is significant when detecting unstable miRNAs. Ultrasensitive signals were also acquired in the following HCR process via continuous assembly of DNA that provides a foundation for trace miRNA analysis. Meanwhile, electrochemical luminescence (ECL) was employed as the high-efficiency signal-producing component. In recent years, ECL achieved revolutionary progress of molecular diagnosis.[41−43] Due to its wide detection range, controlled reaction system, short time consumption, high sensitivity, and signal-to-noise ratio, ECL has gained enormous interests in detection methodology.[44−46] Furthermore, double labeling was executed in ECL probes H1, H3, and H4 to obtain higher ECL intensity and sufficient sensitivity.

2. EXPERIMENTAL SECTION

2.1. Reagents. Streptavidin-labeled magnetic beads were obtained from New England BioLabs (England). Diethylpyrocarbonate (DEPC)-treated water and RNAase inhibitor were obtained from Takara Biotechnology (Dalian) CO., Ltd. PBS (20X solution) and reagents related to electrophoresis were purchased from Shanghai Sangon Biotechnology Co. Ltd. (China). SYBR I and SYBR II were purchased from Invitrogen. All chemicals used were reagent grade and purchased from Sigma-Aldrich and used without further purification except where noted. All oligonucleotides and probes synthesized in this work were purified by Invitrogen (America). ECL signals were recorded using an Elecsys2010 system (Roche, Switzerland). All consumable items were treated with DEPC and sterilized three times.

2.2. Probe Label Process. The DNA probe labeling process consisted of a labeling reaction and purification steps. The amino modified DNA probes (2.5 OD) were first dissolved in sodium borate buffer (pH 8.5, 70 μL). Then, $Ru(bpy)_3^{2+}$-NHS was added until it reached a molecular ratio of 30:1 with the DNA probes. The final volume was set as 100 μL. The DNA probes were incubated with $Ru(bpy)_3^{2+}$-NHS under dark and airtight conditions and achieved sufficient ligation after 12 h of reaction at 37 °C. The ligation products were purified four times using analytical grade ethyl alcohol (80%, 1 mL). In this assay, four cooling and centrifugal sedimentation steps were performed to ensure the purity of the probes.

H1, H3, and H4 were originally tagged with amine groups, which became sites for reacting with $Ru(bpy)_3^{2+}$-NHS. H2 was labeled with biotin. Before construction of the enzyme-free amplification system, both H1 and H2 were subjected to a gradient cooling treatment, which consisted of full denaturation at 95 °C for 5 min, followed by a gradient cooling step that decreased 2 degrees per minute until reaching room temperature. The probes were stored at 4 °C for later use.

2.3. Polyacrylamide Gel Electrophoresis. The amplification products were analyzed using a Bio-Rad slab electrophoresis system (Bio-Rad Laboratories, USA). A 10% native polyacrylamide gel (29:1 acrylamide: bis-acrylamide) was used, and 6 μL samples (4 μL products +1 μL Loading buffer +1 μL stain) were loaded and electrophoresed at room temperature for 45 min at 120 V in 1× Tris-borate-ethylenediaminetetraacetic acid (EDTA) (TBE, 1×), followed by staining with SYBR I and SYBR II. The gels were photographed using a Bio-Rad Digital imaging system.

2.4. Ultrasensitive Hairpin Probe-Based Circulation Reaction. The enzyme-free amplification reaction consisted of hairpin probes (H1, H2, H3, and H4), PBS buffer, RNase inhibitor and DEPC-treated water. The PBS buffer concentration was determined to be 0.8 ×. The RNase inhibitor had a final concentration of 1 U/μL. The entire platform consisted of ultrasensitive enzyme-free amplification and an ECL signal system. The entire set of operation procedures consisted of the enzyme-free DNA circuits, the hybridization chain reaction process, a magnetic bead capturing and cleaning process, and ECL signal detection. The enzyme-free DNA circuit was preferentially initiated with miRNA21 and was employed as a response amplifier for

DOI: 10.1021/acs.biomac.5b00959
Biomacromolecules 2015, 16, 3543−3551

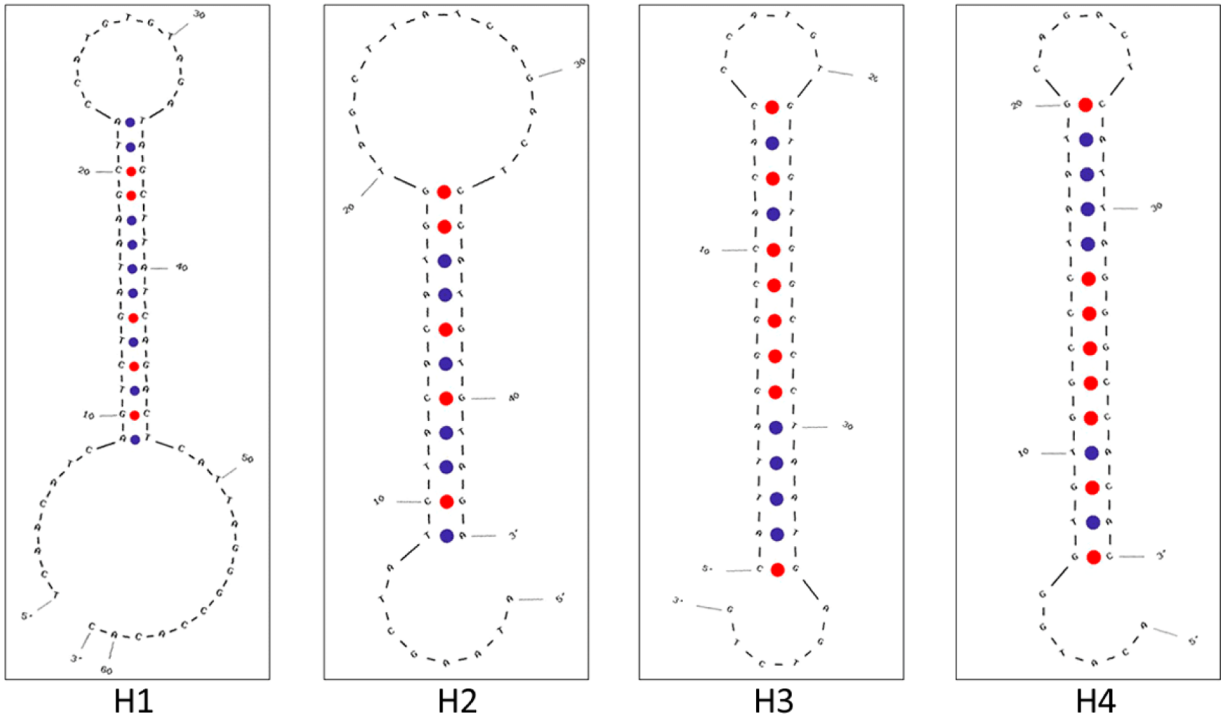

Figure 1. Planar construction of hairpin probes. (H1) Planar construction of H1. The length of the loop structure is 11 nt, and the stem structure is 14 bp. The length of the hairpin unfold breakthrough region is 8 nt. (H2) Planar construction of H2. The length of the loop structure is 14 nt, and the stem structure is 11 bp. (H3) Planar construction of H3. The length of the loop structure is 6 nt, and the stem structure is 14 bp. (H4) Planar construction of H4. The length of the loop structure is 6 nt, and the stem structure is 14 bp.

trace miRNAs and converted to a stable DNA complex (H1+H2) at the initial stage of amplification. Then, the link sequence in H1 (sites 2*, 5 and 6) was freed to trigger the subsequent HCR process. After 1 h of amplification, the products were captured using streptavidin magnetic beads for 30 min at 37 °C. Then, after magnetic separation and three washing steps, the complexes of the amplification products and streptavidin magnetic beads were redissolved in 1× PBS buffer. The amplification products were detected using an Elecsys2010 system, and the ECL signals were recorded.

2.5. Total RNA Extraction. In this work, three tumor cell lines (human lung adenocarcinoma cells, A549; human breast adenocarcinoma cells, MCF-7; and human hepatocellular liver carcinoma cells, HepG2) were selected to evaluate the capability of our platform for the detection of tumor cells. Normal human liver cells (LO2) were chosen as the normal miRNA expression level control group. All cells were cultured in Dulbecco's modified Eagle's medium (DMEM). The medium was supplemented with 10% fetal bovine serum (FBS) and 1% penicillin-streptomycin, and cells were grown in a humidified incubator in 5% CO2 and 95% air at 37 °C. After sufficient growth, the cells were dissociated and counted. The centrifugal cell aggregates were processed with a commercial total RNA extraction kit (Takara Biotechnology (Dalian) Co.), and the extracts were preserved at −80 °C. Absorbance of the cell extracts at 260 nm was also determined. The clinical tumor tissues were provided by the first affiliated hospital of the Jinan University. All tumor tissues were excised from confirmed cancer patients. After detachment of the tumor tissues, a strict freezing protocol was followed by storage at −80 °C. Then, a similar RNA-extraction process was performed using a commercial total RNA extraction kit, and the absorbencies of the extracts at 260 nm were determined.

2.6. Gradient-Cooling Procedure. The process contained a full denaturation at 95 °C for 5 min and a gradient cooling step that drop 5 degrees per minute until cooling down to the room temperature. Then the probes are stored at 4 °C for later use.

3. RESULTS AND DISCUSSION

3.1. Designing and Optimizing Process. In this assay, EFDC, constructed by H1 and H2 probes, was employed as the foremost amplifier to produce a response with trace miRNA and convert it to a stable 'H1+H2' DNA complex at the initial amplification stage. Then, a link segment in H1 was designed to concatenate the subsequent HCR process (constructed by H3 and H4). When the EFDC is activated, the exposed site H1 triggers the continuous HCR process and the continuous probe-assembly of DNA was entirely triggered. After 1 h of amplification, the products were captured using streptavidin magnetic beads for 30 min at 37 °C. Then, after magnetic separation and three washing steps, the complexes of the amplification products and streptavidin magnetic beads were redissolved in 1× PBS buffer. The amplification products were detected using an Elecsys2010 system, and the ECL signals were recorded.

On the basis of the above design, we commenced our investigations by constructing hairpin probe structures (the sequences of the probes are listed in Table S1). The particular design strategies are listed in the Experimental Details section in the Supporting Information. The planar constructions of the hairpin probes are shown in Figure 1. The dynamic parameters of hairpin probes were calculated using Oligo Analyzer 3.1 (listed in Table S2). The experimental details, including synthesis and spectral characterization of the $Ru(bpy)_3^{2+}$-NHS ester, probe label, and characterization are summarized in Figures S1−S6.

To verify the validity of the amplification system, a stepwise proof procedure was performed. First, the validity of the foremost amplifier (EFDC) was verified using 10% polyacrylamide gel electrophoresis (amplifying with 1 pmol of miRNA21). As shown in Figure 2A, a band is apparent in the

DOI: 10.1021/acs.biomac.5b00959
Biomacromolecules 2015, 16, 3543−3551

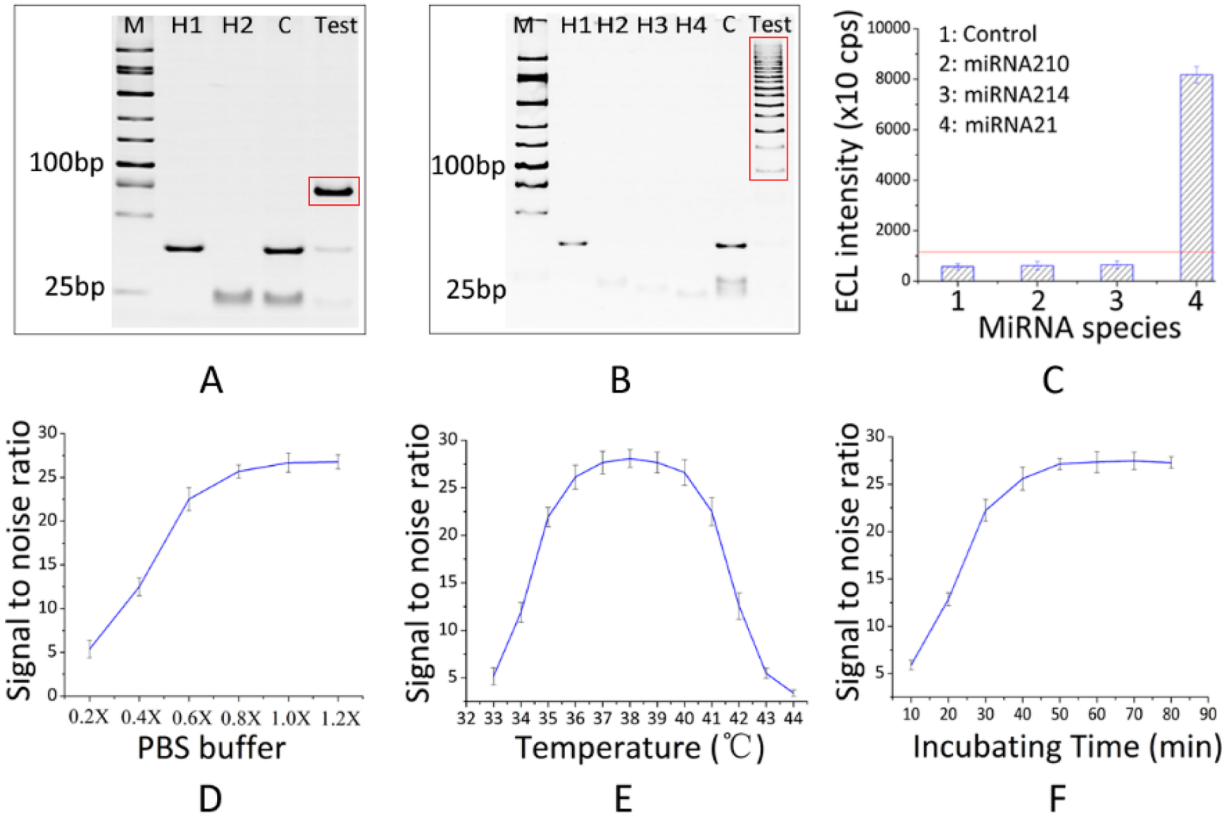

Figure 2. (A) Electrophoresis validity for the foremost amplification process of enzyme-free DNA circuits. The products were analyzed using 10% polyacrylamide gel electrophoresis. Lane M: marker; Lane H1: H1 probe; Lane H2: H2 probe; Lane C: control group; Lane Test: test group with 10 pmol. The expected products are the band marked in red box. (B) Electrophoresis validity for the entire ultrasensitive hairpin probe-based circulation pattern. The amplification system was constructed by H1, H2, H3, and H4 (all set to a final concentration of 50 nM). The incubating temperature was 37 °C. Lanes H1 and H2 are the bands of the H1−H4 probes. Lane C: control group; Lane Test: test group with 10 pmol. The expected products are the stair-stepping band in lane Test (marked in red box). (C) Specificity evaluation of the ultrasensitive hairpin probe-based circulation. The specificity results were obtained at 37 °C following incubation for 1 h. The concentrations of miRNA21, miRNA210, and miRNA214 were all 1 pmol. (D) Evaluation of the effect of PBS buffer concentration on the signal-to-noise ratio. The concentration of miRNA21 was 1 pmol, and the reaction was incubated at 37 °C for 1 h. (E) Evaluation of the effect of incubating temperature on the signal-to-noise ratio. (F) Evaluation of the effect of incubation time on the signal-to-noise ratio. The incubation temperature was 38 °C. The final concentration of PBS was 0.8×.

Test group. Therefore, the validity of the EFDC system was confirmed. In a similar manner, we evaluated the entire ultrasensitive hairpin probe-based circulation system (Figure 2B). The electrophoresis results show that the "Test" group produced stair-step products, which conform to the original design. Thus, the validity of the entire process was demonstrated. Then, a specificity evaluation experiment was conducted. In this experiment, miRNA210, miRNA214, and miRNA21 at an isometric concentration of 1 pmol, were amplified by this platform (the sequences of miRNA21, miRNA210, and miRNA214 are listed in Table S1). The corresponding signals are presented in Figure 2C. The experimental groups of miRNA210 and miRNA214 produced a weak ECL signal that remained at the same level as that of the control group. However, intense signals were observed in the miRNA21 experimental group, indicating that this platform has excellent specificity.

Then, we were interested in the optimization of experimental parameters including ionic strength, incubation time, and temperature. The signal-to-noise ratio was employed as the composite metric to verify wheher these conditions were appropriate. It is generally acknowledged that salt ions in solution can neutralize the negative charges of nucleic acids,[47] which promotes DNA hybridization and hairpin structures. Thus, an appropriate ionic strength could have a positive effect on the stability of hairpin structures and enhance the sensitivity and specificity of the assay. Higher ionic strengths can promote a more stable hairpin-structure for all of the probes and have a positive effect on the specificity but not on the sensitivity. Alternatively, a lower ionic strength would increase the sensitivity but not the specificity. To achieve the ionic strength required to reach equilibrium, we investigated the effect of phosphate buffered saline (PBS) buffer concentrations on the signal-to-noise ratio to produce the most effective salt ion reaction environment. This effect was evaluated by setting the PBS concentrations to 0.2× , 0.4×, 0.6×, 0.8×, 1.0×, and 1.2×. An equivalent amount of miRNA21 (1 pmol) was also added in the amplification system. As shown in Figure 2D, the signal-to-noise ratio increased as the concentration of PBS buffer increased. When the concentration of the PBS buffer reached 0.8×, the signal-to-noise ratio maintained a stable level. Further addition of PBS buffer led to no further increase in the signal-to-noise ratio. This result demonstrates the promoting effect of salt ions in solution on DNA hybridization and the fabrication of hairpin structures. Thus, we chose 0.8× PBS buffer for the platform.

Temperature is an inherently important parameter in reaction kinetics that determines the probability of molecule

DOI: 10.1021/acs.biomac.5b00959
Biomacromolecules 2015, 16, 3543−3551

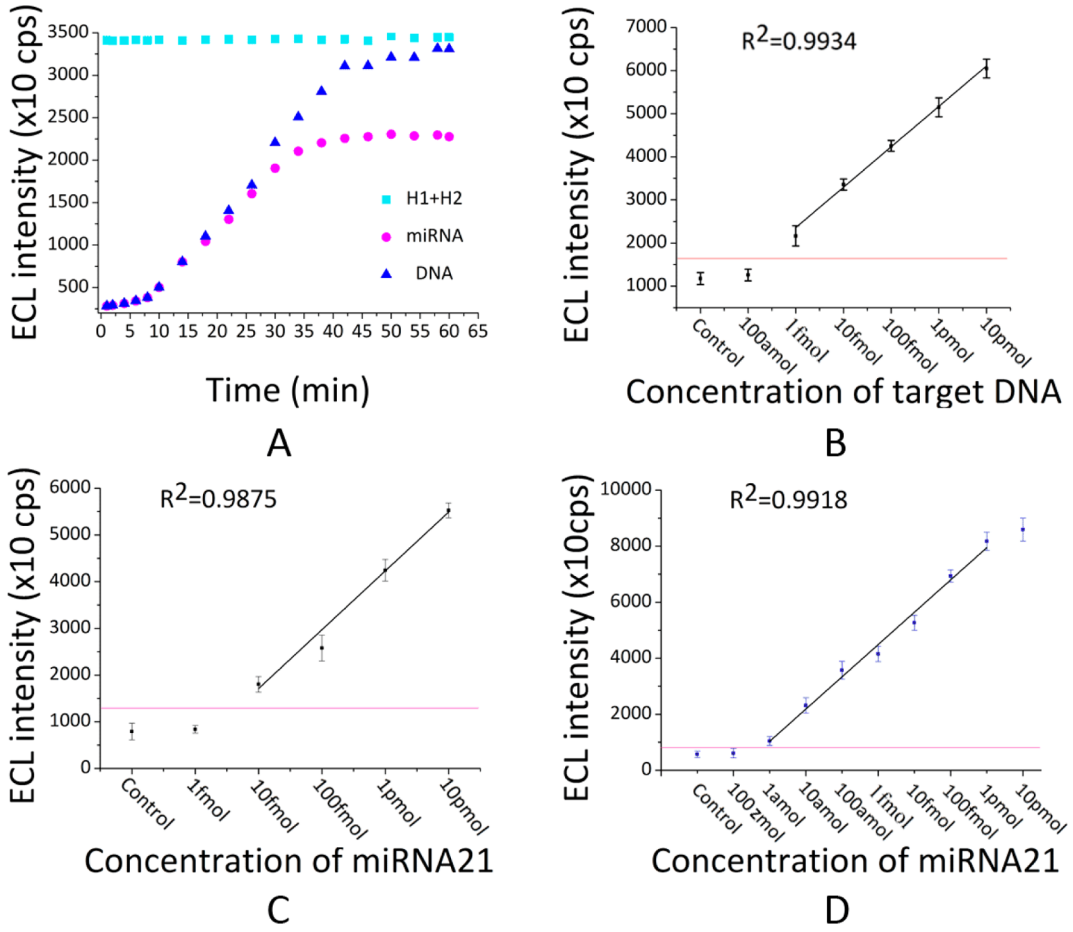

Figure 3. Comparisons of enzyme-free DNA circuits, the hybridization chain reaction and ultrasensitive enzyme-free amplification. (A) The verification experiments of the analyte stability-dependent amplification efficiency in enzyme-free DNA circuits. The concentrations of target DNA and miRNA were all 1 pmol, and RNase was not eliminated. The final concentrations of H1 and H2 were 50 nM. The sequence of "DNA" used here was equal to miRNA21 (uracil was changed to thymine). (B) The sensitivity experiments of the hybridization chain reaction. A segment of the ideal DNA target (link segment) was compounded to activate the designed HCR system consisting of H3 and H4 (50 nM). (C) The sensitivity experiments of enzyme-free DNA circuits. (D) The sensitivity experiments of ultrasensitive enzyme-free amplification pattern. The entire process was executed under optimized conditions (37 °C, 0.8× PBS and 1 h of incubation).

collisions.[48] In this work, we found that the incubation temperature is the key factor that influences the stability and interactions of the hairpins. At lower temperatures, hairpin probes cannot attain a sufficient collision probability, greatly reducing the formation of amplification products. Conversely, the specificity of this platform is diminished by higher incubation temperatures due to the decreased stability and integrity of hairpin probes. To determine the optimal incubation temperature, experiments were conducted at a temperature range of 33−44 °C, and the signal-to-noise ratios were assessed. As shown in Figure 2E, a peak value for the signal-to-noise ratio was obtained at 38 °C. Consequently, 38 °C was designated as the optimum incubation temperature. The results also affirmed the correctness of the above descriptions. The lower and higher incubation temperature groups produced inferior signal-to-noise ratios. Furthermore, the reaction time is an important parameter in reaction kinetics.[31] Sufficient incubation time would produce an efficient amplification. To further improve this platform, incubation time optimization experiments were performed using the signal-to-noise ratio as the evaluation criterion. The ECL signals were detected at different incubation time points, and shown in Figure 2F. The signal-to-noise ratio increased with increasing incubation times. At 60 min, the signal-to-noise ratio became stable. Therefore, 60 min was chosen as the optimal incubation time.

3.2. Comparisons of EFDC, HCR and Ultrasensitive Hairpin Probe-Based Circulation. The sensitivities for the EFDC, HCR, and the ultrasensitive hairpin probe-based circulation were compared under identical conditions. We primarily evaluated the analyte stability-dependent amplification efficiency of the EFDC. In this assay, the ECL intensity using 50 nM H1+H2 complex was determined within a time range of 1 h (The H1+H2 complex was acquired by the denaturation and gradient cooling procedure). A nearly constant ECL intensity of approximately 30 000 cps was obtained using the 50 nM H1+H2 complex, as shown in Figure 3A. The ECL intensities generated by miRNA and DNA targets (the sequence of DNA target was equal to miRNA, uracil was changed to thymine) were then determined at regular time points. In the initial phase (the first 10 min), the ECL intensities were approximately the same for both groups, after which time higher results were obtained with the DNA group. The ECL intensity for the miRNA group reached a plateau of approximately 20 000 cps at 35 min. However, the ECL intensity for the DNA target group rose linearly until 50 min, at

DOI: 10.1021/acs.biomac.5b00959
Biomacromolecules 2015, 16, 3543−3551

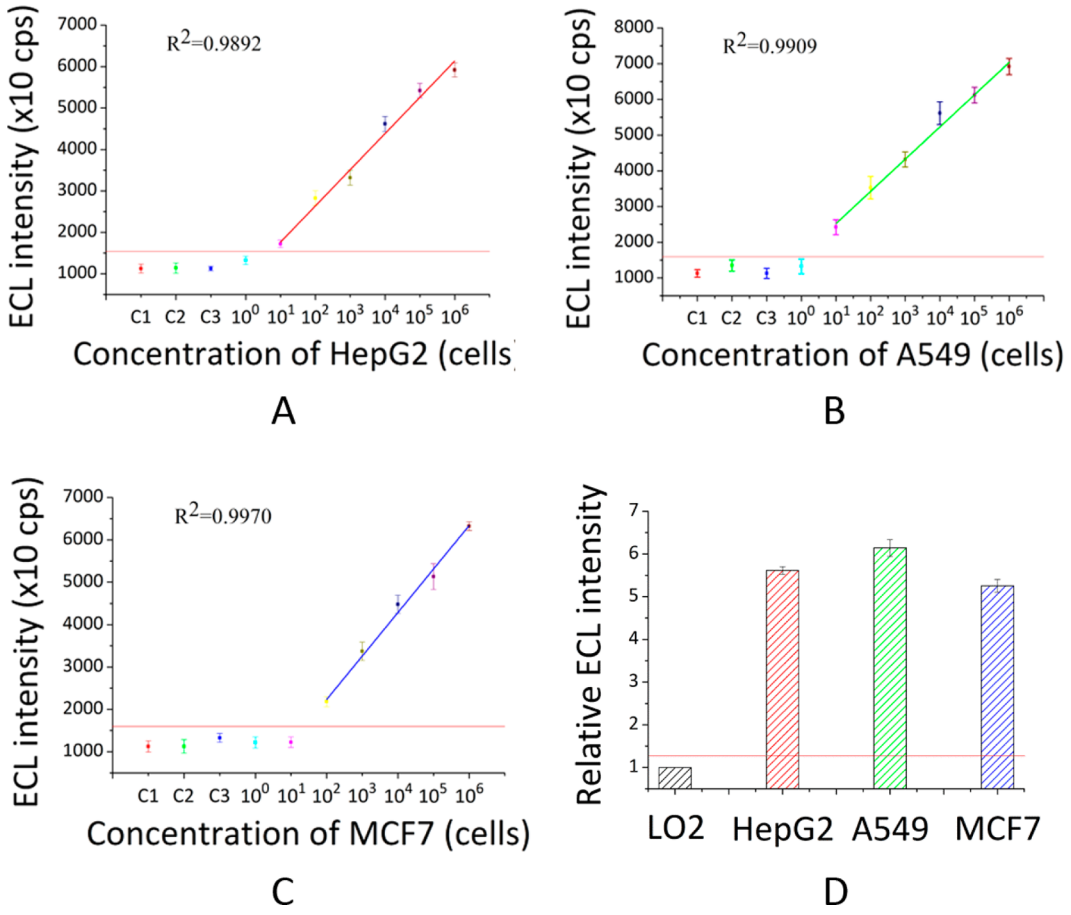

Figure 4. Sensitivity experiments for tumor cell lines and data analysis. (A) Sensitivity experiments for HepG2 cells and data analysis. (B) Sensitivity experiments for A549 cells and data analysis. (C) Sensitivity experiments for MCF-7 cells and data analysis. (D) The miRNA21 expression differences between human normal cell lines and tumor cell lines. All cells were cultured in Dulbecco's modified Eagle's medium (DMEM). The medium was supplemented with 10% fetal bovine serum (FBS), and cells were grown in a humidified incubator in 5% CO_2 and 95% air at 37 °C. C1: LO2 cell line; C2: HUVEC cell line; C3: HBE cell line. The tumor cell lines were processed, and the cells were counted before extraction. The rigorous cell counting process was executed to ensure the cell count was equal in the comparisons of expression differences.

which point it became constant at the same level obtained with the H1−H2 complex group. Thus, we conclude that the degradation of the miRNA seriously reduced the amplification efficiency of the EFDC process. In the terminal phase of the amplification reaction, the amplification efficiency in the miRNA group was significantly reduced, which demonstrated the analyte stability-dependent amplification efficiency of the EFDC. This assay proceeded with simple steam sterilization. No DEPC-treated process and RNase inhibitor was involved. Besides, we artificially introduced RNases in the reaction system to support mRNA degradation causes the difference in the results. The results in Figure S7 were in accordance with the results recorded in Figure 3A.

We then separated the entire amplification process into two components, which were composed of independent HCR and EFDC systems. Primarily, the sensitivity experiment with the independent amplification process (HCR) was performed to demonstrate the initial concentration-dependent effect. To rule out interference by miRNA degradation elements, we synthesized ideal DNA targets to inspect the designed HCR system. The concentrations of ideal DNA targets ranged from 1 fmol to 10 pmol. The ECL signals were observed and are shown in Figure 3B. An unsatisfactory sensitivity of 1 fmol was obtained under certain conditions (37 °C, 50 nM H3 and H4, 1 h). Lower amounts of DNA targets could not evoke a recognizable response with the HCR system. Thus, the previous assumption was adequately verified that HCR strongly relies on the initial concentration of analyte. In addition, a sensitivity evaluation experiment for the EFDC was performed. As shown in Figure 3C, the constructed EFDC process had an unsatisfactory sensitivity of 10 fmol, which was lower by an order of magnitude.

Afterward, we performed sensitivity experiments to evaluate the sensitivity of the ultrasensitive hairpin probe-based circulation platform under the optimized conditions. Here, the concentration of miRNA21 ranged from 100 zmol to 100 pmol. The ECL signals were measured and are shown in Figure 3D. The ECL intensity decreased synchronously with the reduction of miRNA21. When the concentration of miRNA21 reached 100 zmol, the ECL intensity became coincident with that of the control group. Conversely, the group with 1 amol miRNA21 exhibited an obvious enhancement compared with the control group. The signal-to-noise ratio for the 1 amol group reached 5.317 ± 0.803, which demonstrated that this ultrasensitive hairpin probe-based circulation achieved a high sensitivity of 1 amol. Thus, this platform exhibited the highest amplification efficiency in the enzyme-free amplification mode and could meet the demands required for miRNA trace analysis. We demonstrated that this platform achieved good linearity (R^2 value: 0.9918) from 1 amol to 1 pmol (see Figure

DOI: 10.1021/acs.biomac.5b00959
Biomacromolecules 2015, 16, 3543−3551

3D). The ECL signal became saturated when the concentration of miRNA21 was increased to 10 pmol. By comparison, the sensitivity of the ultrasensitive hairpin probe-based circulation was 3 or 4 orders of magnitude higher than that of the individual EFDC and HCR processes. Meanwhile, we executed the intensity-overtime curves for HCR, EFDC, and combined systems for further proof of ultrasensitive hairpin probe-based circulation works faster. The results in Figure S10 provided full proof for the above reasoning. All the amplification system were executed in the parallel condition of 37 °C, 0.8× PBS and 1 h of incubation. The target of these three systems was identical to that of miRNA21. The DNA probes of EFDC and the combined system were equal to the sequence used in manuscript. The DNA probe of HCR was listed in Table S5. These result all demonstrated that the integrated ultrasensitive hairpin probe-based circulation pattern exhibited excellent performance.

3.3. Sensitivity Results and miRNA21 Expression Level Comparisons in Tumor Cells. In this section, three tumor cell lines (a hepatic carcinoma cell line, HepG2; a lung carcinoma cell line, A549; and a breast adenocarcinoma cell line, MCF-7) with high expression levels of miRNA21[49−51] were selected to investigate the capability of ultrasensitive hairpin probe-based circulation for tumor cell detection. The cell samples were processed using a total RNA extraction kit after cell counting. The sensitivities were explored by setting the cell concentrations from 10^0 to 10^6 cells. As shown in Figure 4A,B,C, the sensitivities for HepG2, A549, and MCF-7 cells reached 10, 10, and 100 cells, respectively, and linear regression analyses of the sensitivity data yielded R^2 values of 0.9892, 0.9909, and 0.9970, respectively. Thus, this platform is capable of performing quantitative detection of miRNA21 in tumor cell lines.

In addition, the miRNA21 expression differences between human normal cells (human normal hepatocyte, LO2) and tumor cells (A549, MCF-7, and HepG2) were compared. All cell concentrations were set to 106 cells for each group. ECL signals were recorded and are shown in Figure 4D. The LO2 cell line was employed as the normal expression quantity control group for miRNA21. The ECL intensity of LO2 cells was artificially defined as 1 unit for characterization of miRNA21 expression levels, and the ECL intensity ratio of tumor cells to normal cells (called relative ECL intensity) was employed as the standard for miRNA21 expression levels. The results demonstrated different miRNA21 expression levels in the three tumor cell lines, and the miRNA21 expression levels in tumor cells were obviously greater than those in normal human cells. The results are also in accordance with the findings in our qRT-PCR experiments (shown in Figure S8 and S9, U6 small nuclear RNA (snRNA) was employed as the universal endogenous control and the relative expression was calculated by the equation: Fold change = $2^{-\Delta\Delta Ct}$, the DNA sequences and details for qRT-PCR are listed in Tables S3 and S4).

3.4. Detection of Clinical Tumor Tissues. Three types of clinical tumor tissues (corresponding to the selected tumor cell lines) were selected for further evaluation of this platform. Clinical tumor tissues are generally complex, which presents serious challenges for diagnosis. Thus, an excellent platform of tumor molecular diagnosis should cope with the complex physiological environment of tumor tissues. Here, three types of clinical tumor tissues were derived from patients with confirmed lung adenocarcinoma, breast adenocarcinoma, or hepatocellular carcinoma. These tumor tissues were pretreated with liquid nitrogen and ground into a paste, and the total RNA was extracted using a commercial kit. In this detection assay, 60 clinical tumor samples were tested, and each experimental group contained extractions from 1 g of tumor tissue. The experimental results shown in Figure 5A,B,C indicate that 50

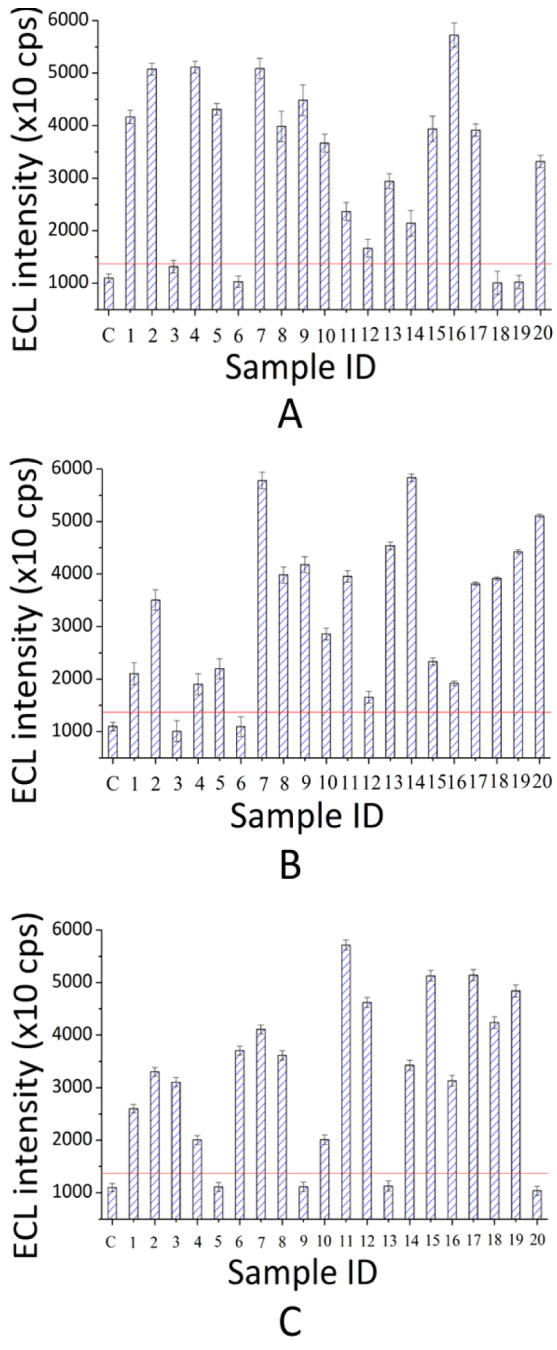

Figure 5. Tests of tumor tissues with ultrasensitive enzyme-free amplification. (A) Tests of human lung adenocarcinoma tissues. (B) Tests of human breast adenocarcinoma tissues. (C) Tests of human hepatocellular carcinoma tissues. All tumor tissues were derived from confirmed patients, pretreated with liquid nitrogen, and ground to a paste; then the total RNA was extracted using a commercial kit. The detection rate was quantified by comparing the ECL signal of the tumor samples with normal tissues (liver tissue from surgery), which is the control group of this assay. The threshold was set as the average ECL intensity + 3 times the error bar.

DOI: 10.1021/acs.biomac.5b00959
Biomacromolecules 2015, 16, 3543−3551

experimental groups produced positive signals and had high expression levels of miRNA21. Furthermore, a high detection rate of 83% was achieved for the tumor tissues. The detection rate was quantified by comparing the ECL signal of the tumor samples with normal tissues (liver tissue from surgery) which is the control group of this assay. The threshold was set as the average ECL intensity + 3 times the error bar. In consideration of the intertwining between tumor tissues and normal tissues, a higher accuracy of detection could be obtained by increasing the sample dosage and by processing multiple samples of tumor tissues. Meanwhile, the qPCR assay is also executed for tumor tissues. The results are added in Figures S11 to S16, and the details are listed in Tables S6 to S8. U6 small nuclear RNA (snRNA) was also employed as the universal endogenous control, and the relative expression was calculated by the equation: Fold change = $2^{-\Delta\Delta Ct}$. The results of relative expression levels were basically in accordance with the ultrasensitive hairpin probe-based circulation. It indicated that this platform has the potential to be a versatile strategy for tumor molecular diagnosis or related research.

4. CONCLUSIONS

We developed an ultrasensitive hairpin probe-based circulation reaction for continuous assemble of DNA probe. This platform integrated and improved the classical EFDC and HCR processes. In the analysis of standard miRNAs, 1 amol sensitivities and satisfactory specificities were obtained. Compared with EFDC and HCR, the sensitivity with the ultrasensitive hairpin probe-based circulation pattern was 3 to 4 orders of magnitude greater. Furthermore, the excellent performance of this platform was also demonstrated by the detection of tumor cells. The sensitivities obtained with HepG2, A549, and MCF-7 cells were 10, 10, and 100 cells, respectively. A definitive high detection rate of 83% was achieved for tumor tissues. In conclusion, three advantages were achieved by the use of this platform. First, this platform attained a high sensitivity of 1 amol, demonstrating improved performance in trace analysis without the participation of enzymes. Second, simplified and isothermal reaction conditions were achieved. The entire process was conducted in PBS solution. Third, this platform is compatible with the complex physiological environment of tumor cells and tissues, and it yields high sensitivities. A preferable detection ratio (approximately 83%) was also achieved. Thus, this platform has the potential to be a versatile strategy for tumor molecular diagnosis and related research.

■ ASSOCIATED CONTENT

Supporting Information

The Supporting Information is available free of charge on the ACS Publications website at DOI: 10.1021/acs.biomac.5b00959.

Characterization and supplementary data (PDF)

■ AUTHOR INFORMATION

Corresponding Authors

*E-mail: zhouxm@scnu.edu.cn; Phone: (+86-20) 8521-0089; Fax: (+86-20) 8521-6052.

*E-mail: xingda@scnu.edu.cn.

Notes

The authors declare no competing financial interest.

■ ACKNOWLEDGMENTS

This research was supported by the National Basic Research Program of China (2010CB732602), the National Natural Science Foundation of China (21475048), the National Science Fund for Distinguished Young Scholars of Guangdong Province (2014A030306008) and the Program of the Pearl River Young Talents of Science and Technology in Guangzhou, China (2013J2200021).

■ REFERENCES

(1) Breaker, R. R. *Nature* **2004**, *432*, 838−845.

(2) Dykxhoorn, D. M.; Novina, C. D.; Sharp, P. A. *Nat. Rev. Mol. Cell Biol.* **2003**, *4*, 457−467.

(3) Krützfeldt, J.; Poy, M. N.; Stoffel, M. *Nat. Genet.* **2006**, *38*, S14−S19.

(4) Bartel, D. P. *Cell* **2004**, *116*, 281−297.

(5) Baltimore, D.; Boldin, M. P.; O'Connell, R. M.; Rao, D. S.; Taganov, K. D. *Nat. Immunol.* **2008**, *9*, 839−845.

(6) Ambros, V. *Nature* **2004**, *431*, 350−355.

(7) Cissell, K. A.; Rahimi, Y.; Shrestha, S.; Hunt, E. A.; Deo, S. K. *Anal. Chem.* **2008**, *80*, 2319−2325.

(8) Zhu, X.; Zhou, X.; Xing, D. *Chem. - Eur. J.* **2013**, *19*, 5487−94.

(9) Zhou, Y.; Huang, Q.; Gao, J.; Lu, J.; Shen, X.; Fan, C. *Nucleic Acids Res.* **2010**, *38* (15), e156.

(10) Cissell, K. A.; Shrestha, S.; Deo, S. K. *Anal. Chem.* **2007**, *79*, 4754−4761.

(11) Cho, W. C. *Mol. Cancer* **2007**, *6*, 60−67.

(12) Vogel, B.; Keller, A.; Frese, K. S.; Kloos, W.; Kayvanpour, E.; Sedaghat-Hamedani, F.; et al. *Clin. Chem.* **2013**, *59*, 410−418.

(13) Lee, R. C.; Feinbaum, R. L.; Ambros, V. *Cell* **1993**, *75*, 843−854.

(14) Lu, J.; Getz, G.; Miska, E. A.; Alvarez-Saavedra, E.; Lamb, J.; Peck, D.; Sweet-Cordero, A.; Ebert, B. L.; Mak, R. H.; Ferrando, A. A.; et al. *Nature* **2005**, *435*, 834−838.

(15) Garzon, R.; Calin, G. A.; Croce, C. M. *Annu. Rev. Med.* **2009**, *60*, 167−179.

(16) Jou, A. F.j.; Lu, C. H.; Ou, Y.; Wang, S. S.; Hsu, S. L.; Willner, I.; Ho. *J. Am. Chem. Sci.* **2015**, *6*, 659−665.

(17) He, H. Z.; Leung, K. H.; Wang, W.; Chan, D. S.H.; Leung, C. H.; Ma, D. L. *Chem. Commun.* **2014**, *50*, 5313−5315.

(18) Lu, L.; Shiu-Hin Chan, D.; Kwong, D.W. J.; He, H. Z.; Leung, C. H.; Ma, D. L. *Chem. Sci.* **2014**, *5*, 4561−4568.

(19) Leung, K. H.; He, H. Z.; He, B.; Zhong, H. J.; Lin, S.; Wang, Y. T.; Ma, D. L.; Leung, C. H. *Chem. Sci.* **2015**, *6*, 2166−2171.

(20) Willner, I.; Shlyahovsky, B.; Zayats, M.; Willner, B. *Chem. Soc. Rev.* **2008**, *37*, 1153−1165.

(21) Liu, J.; Lu, Y. *Angew. Chem., Int. Ed.* **2007**, *46*, 7587−7590.

(22) Brown, C. W.; Lakin, M. R.; Horwitz, E. K.; Fanning, M. L.; West, H. E.; Stefanovic, D.; Graves, S. W. *Angew. Chem., Int. Ed.* **2014**, *53*, 7183−7187.

(23) Hermann, T.; Patel, D. J. *Science* **2000**, *287*, 820−825.

(24) Mayer, G. *Angew. Chem., Int. Ed.* **2009**, *48*, 2672−2689.

(25) Zheng, A. X.; Li, J.; Wang, J. R.; Song, X. R.; Chen, G. N.; Yang, H. H. *Chem. Commun.* **2012**, *48*, 3112−3114.

(26) Zheng, A. X.; Wang, J. R.; Li, J.; Song, X. R.; Chen, G. N.; Yang, H. H. *Biosens. Bioelectron.* **2012**, *36*, 217−221.

(27) Li, B.; Jiang, Y.; Chen, X.; Ellington, A. D. *J. Am. Chem. Soc.* **2012**, *134*, 13918−13921.

(28) Seelig, G.; Soloveichik, D.; Zhang, D. Y.; Winfree, E. *Science* **2006**, *314*, 1585−1588.

(29) Yin, P.; Choi, H. M.; Calvert, C. R.; Pierce, N. A. *Nature* **2008**, *451*, 318−322.

(30) Qian, L.; Winfree, E. *Science* **2011**, *332*, 1196−1201.

(31) Li, B.; Chen, X.; Ellington, A. D. *Anal. Chem.* **2012**, *84*, 8371−8377.

(32) Chen, J.; Zhou, X.; Zeng, L. *Chem. Commun.* **2013**, *49*, 984−986.

(33) Liao, Y.; Huang, R.; Ma, Z.; Wu, Y.; Zhou, X.; Xing, D. *Anal. Chem.* **2014**, *86*, 4596−4604.

DOI: 10.1021/acs.biomac.5b00959
Biomacromolecules 2015, 16, 3543−3551

(34) Li, B.; Ellington, A. D.; Chen, X. *Nucleic Acids Res.* **2011**, *39*, e110−e110.
(35) Zheng, A. X.; Li, J.; Wang, J. R.; Song, X. R.; Chen, G. N.; Yang, H. H. *Chem. Commun.* **2012**, *48*, 3112−3114.
(36) Huang, R.; Liao, Y.; Zhou, X.; Xing, D. *Anal. Chim. Acta* **2015**, *888*, 162−172.
(37) Huang, J.; Su, X.; Li, Z. *Anal. Chem.* **2012**, *84*, 5939−5943.
(38) Dirks, R. M.; Pierce, N. A. *Proc. Natl. Acad. Sci. U. S. A.* **2004**, *101*, 15275−15278.
(39) Evanko, D. *Nat. Methods* **2004**, *1*, 186−187.
(40) Dirks, R.; Pierce, N. A. US Patent US 7,632,641, 2009
(41) Sardesai, N.; Kadimisetty, K.; Faria, R.; Rusling, J. *Anal. Bioanal. Chem.* **2013**, *405*, 3831−3838.
(42) Richter, M. M. *Chem. Rev.* **2004**, *104*, 3003−3036.
(43) Delaney, J. L.; Hogan, C. F.; Tian, J.; Shen, W. *Anal. Chem.* **2011**, *83*, 1300−1306.
(44) Liu, T.; Chen, X.; Hong, C. Y.; Xu, X. P.; Yang, H. H. *Microchim. Acta* **2014**, *181*, 731−736.
(45) Cheng, Y.; Lei, J.; Chen, Y.; Ju, H. *Biosens. Bioelectron.* **2014**, *51*, 431−436.
(46) Wu, X.; Chai, Y.; Yuan, R.; Su, H.; Han, J. *Analyst* **2013**, *138*, 1060−1066.
(47) Tan, Z. J.; Chen, S. J. *Biophys. J.* **2006**, *90*, 1175−1190.
(48) Pilling, M. J.; Seakins, P. W. *Reaction Kinetics*; Oxford University Press: Oxford, U.K., 1996.
(49) Wang, Z. X.; Bian, H. B.; Wang, J. R.; Cheng, Z. X.; Wang, K. M.; De, W. *J. Surg. Oncol.* **2011**, *104*, 847−851.
(50) Calin, G. A.; Sevignani, C.; Dumitru, C. D.; Hyslop, T.; Noch, E.; Yendamuri, S.; Shimizu, M.; Rattan, S.; Bullrich, F.; Negrini, M.; Croce, C. M. *Proc. Natl. Acad. Sci. U. S. A.* **2004**, *101*, 2999−3004.
(51) Iorio, M. V.; Ferracin, M.; Liu, C. G.; Veronese, A.; Spizzo, R.; Sabbioni, S.; Magri, E.; Pedriali, M.; Fabbri, M.; Campiglio, M.; Ménard, S.; Palazzo, J. P.; Rosenberg, A.; Musiani, P.; Volinia, S.; Nenci, I.; Calin, G. A.; Querzoli, P.; Negrini, M.; Croce, C. M. *Cancer Res.* **2005**, *65*, 7065−7070.

DOI: 10.1021/acs.biomac.5b00959
Biomacromolecules 2015, 16, 3543−3551